

7.1 DERIVATION OF COMPONENT AEROSOL DIRECT RADIATIVE FORCING FOR THE CLEAR SKY BY COMBINING SATELLITE MEASUREMENT AND MODEL SIMULATIONS

Tom X.-P. Zhao^{1,2*}, Hongbin Yu^{3,4}, Istvan Laszlo², and Mian Chin³

¹CICS/ESSIC/UMD, College Park, MD 20742, USA

²NOAA / NESDIS / STAR, Camp Springs, MD 20746, USA

³Laboratory for Atmospheres, NASA/GSFC, Greenbelt, MD 20771, USA

⁴Goddard Earth Science and Technology Center, UMBC, Baltimore, MD 21250, USA

1. INTRODUCTION

Satellite observations have actively joined traditional model calculations for the estimation of global aerosol direct radiative effect (DRE) (Yu et al., 2005) and observed size information (such as the Ångström coefficient and the fine-model fraction) has also been utilized to discriminate ensemble anthropogenic aerosol from natural aerosol in order to determine the global radiative effect of anthropogenic aerosols (Kaufman et al, 2005), termed as the aerosol direct radiative forcing (DRF). However, it is still difficult to use satellite observations alone to further discriminate aerosols into more detailed components (such as sea salt, dust, sulfate, back and organic carbons) over the globe as well as to derive their direct radiative effect/forcing (DRE/DRF). Since aerosol DRE/DRF from different aerosol components can be very different (e.g., even the sign of the forcing can be reversed), an accurate estimation of component aerosol DRE/DRF becomes important and deserves to be explored. Here, we propose a new approach of combining satellite Clouds and the Earth's Radiant Energy System (CERES) measured aerosol DRE with the optical thickness fractions of major aerosol components from the NASA Goddard Global Chemistry Aerosol Radiation and Transport (GOCART) model to derive the component aerosol DRE/DRF over global oceans.

2. SATELLITE AND MODEL PRODUCTS

In the proposed analysis, aerosols are divided into five major components, black carbon (BC), organic matter (OM), sulfate (SU), dust (DU), and sea salt (SS). The total aerosol optical thickness (AOT or τ) is the summation of component AOTs ($\tau_{TOT} = \tau_{BC} + \tau_{OM} + \tau_{SU} + \tau_{DU} + \tau_{SS} = \sum_{i=1} \tau_i$).

- *Corresponding author address:* Tom X.-P. Zhao, CICS/ESSIC, University of Maryland, College Park, MD 20742, USA; email: Xuepeng.Zhao@noaa.gov

As a first order approximation, BC, OM and SU are further grouped as anthropogenic aerosols ($\tau_{AN} = \tau_{BC} + \tau_{OM} + \tau_{SU}$) and DU and SS are grouped as natural aerosols ($\tau_{NA} = \tau_{DU} + \tau_{SS}$). The fractions (r_i) of component aerosol optical thicknesses are determined by the relationship $r_i = \tau_i / \tau_{TOT}$ ($\tau_i = \tau_{BC}, \tau_{OM}, \tau_{SU}, \tau_{DU}, \tau_{SS}, \tau_{AN}$, and τ_{NA}). The aerosol optical parameter that will be used to derive aerosol DRE/DRF in the proposed approach is the AOT at $0.55\mu\text{m}$.

The global MODerate Resolution Imaging Spectroradiometer (MODIS) AOTs aggregated to the CERES single scanner footprint (SSF) was used, which was taken from the daytime Edition-1A Terra/CERES-MODIS SSF data for the year 2001. The SSF aerosol data were grided into $1^\circ \times 1^\circ$ daily product and a detailed description can be founded in Zhao et al. (2005a, b). Daily AOT values from the GOCART model (Chin et al., 2000, 2002) and an optimum interpolation approach with the Kalman-Bucy filter (Yu et al., 2003) were used to fill the gaps of SSF-MODIS AOT due to the limitation of MODIS aerosol retrieval (such as over bright surfaces and sunglint areas). The merged daily AOTs were further averaged to obtain monthly mean values. The merged daily and monthly aerosol optical thicknesses (τ_{TOT}) were then partitioned into major aerosol components (τ_i , $i=BC, OM, SU, DU, SS, AN, NA$) by using the component fractions (r_i) from the GOCART model with $\tau_i = r_i (\text{GOCART}) \times \tau_{TOT}$ (merged).

3. METHODOLOGY

A two-step approach is proposed to derive the component aerosol DRE/DRF. The first step is to derive total aerosol DRE at the top of atmosphere (TOA) using an approach proposed by Loeb and Kato (2002). The TOA aerosol DRE for a given day (d) and given location at latitude (θ) and longitude (φ) is defined as the following:

$$\Delta F(d, \theta, \varphi) = \bar{F}^{na}(d, \theta, \varphi) - \bar{F}^a(d, \theta, \varphi), \quad (1)$$

where $\bar{F}^{na}(d, \theta, \varphi)$ and $\bar{F}^a(d, \theta, \varphi)$ are the daily average SW fluxes in the absence and presence of aerosols, respectively. The $\Delta F(d, \theta, \varphi)$ is determined

from instantaneous SSF TOA fluxes that are converted to daily averages over $1^\circ \times 1^\circ$ grids.

To determine $\bar{F}^a(d, \theta, \varphi)$, the instantaneous TOA fluxes are converted to a daily average by applying diurnal albedo model for ocean surface to estimate what the reflected SW flux would be at all local times of the day assuming no changes in aerosol or surface properties, and averaging these fluxes over 24 hours (Loeb and Kato, 2002; Loeb and Manalo-Smith, 2005). A simple regression procedure (Loeb and Kato, 2002) is used to derive $\bar{F}^{na}(d, \theta, \varphi)$. Specifically, instantaneous SSF TOA fluxes are plotted against the above merged AOTs at $0.55\mu\text{m}$ in 1° solar zenith angle increments. The regression for each 1° solar zenith angle interval is extrapolated to zero aerosol optical thickness and the corresponding solar flux is used for the “no aerosol” flux. A sixth-order polynomial fit is applied to the “no aerosol” fluxes for all of the 1° solar zenith angles. The $\bar{F}^{na}(d, \theta, \varphi)$ value for a given area is then determined by averaging the fluxes retrieved from the polynomial fit. The value of $\Delta F(d, \theta, \varphi)$ is further averaged to obtain monthly, seasonal, and annual means, which are the focus of this study.

The second step is to determine component aerosol DRE/DRF. According to Boucher et al. (1998), Boucher and Tanré (2000), and Bellouin et al. (2003), the DRE/DRF of non- or weakly-absorbing aerosols is, to a good approximation, proportional to $(e^{-\tau}-1)$. Based on this empirical relationship, we partition $\Delta F(d, \theta, \varphi)$ first into a natural component $\Delta F_{NA}(d, \theta, \varphi)$ according to,

$$\Delta F_{NA}(d, \theta, \varphi) = \Delta F(d, \theta, \varphi) \times (e^{-\tau_{na}} - 1) / (e^{-\tau} - 1), \quad (2)$$

due to a weak absorption of the natural aerosols (SS+DU). This relationship implicitly assumes that the forcing efficiency (or forcing per unit of AOT) of natural component at TOA is equal to that of total aerosols. This assumption is justified by some recent research findings. For example, according to Zhang et al. (2005a,b), small fine mode fraction ($\eta < 0.6$) relates to large particles such as sea salt and dust particles (or natural aerosols). Their estimated forcing efficiency for these particles is about 5% higher (more negative) than the average (or total) aerosol forcing efficiency. Large fine mode fraction ($\eta > 0.8$) relates to smaller particles like smoke and pollutant aerosols (or anthropogenic aerosols). Their estimated forcing efficiency for these particles is about 10% lower (less negative) than the average aerosol forcing efficiency. Kaufman et al. (2005) found that forcing efficiency of more absorbing aerosols such as smoke particles is about 20% on average lower (less negative) than the average aerosol forcing efficiency with an uncertainty of about 30%. To avoid the relatively large error

caused by our assumption for absorbing aerosols, we propose to further derive anthropogenic component $\Delta F_{AN}(d, \theta, \varphi)$ by subtracting the natural component from the total forcing, i.e. $\Delta F_{AN}(d, \theta, \varphi) = \Delta F(d, \theta, \varphi) - \Delta F_{NA}(d, \theta, \varphi)$. Thus, the uncertainty in the forcing of anthropogenic component is reduced and is close to that of natural component.

Using the same procedure, $\Delta F(d, \theta, \varphi)$ can be partitioned into a sea salt component $\Delta F_{SS}(d, \theta, \varphi)$, a sulfate component $\Delta F_{SU}(d, \theta, \varphi)$, a dust component $\Delta F_{DU}(d, \theta, \varphi)$, and an organic matter component $\Delta F_{OM}(d, \theta, \varphi)$ since they are either non-absorbing or weakly-absorbing. The uncertainty in the partition of sulfate component should be close to sea salt component ($\sim 5\%$) due to their similar non-absorbing characteristics. The same assumption is also applied to organic matter and dust component with an uncertainty of about 10% due to their similar weakly-absorbing characteristics. Subtracting these components from $\Delta F(d, \theta, \varphi)$ and the remaining is considered as a black carbon component $\Delta F_{BC}(d, \theta, \varphi)$. If we assume the uncertainties in all subtracted components are independent, the square root for the addition of squares of these independent uncertainties can be considered as the uncertainty in $\Delta F_{BC}(d, \theta, \varphi)$ ($\sim 16\%$). This large uncertainty is not unexpected by subtracting two big terms to derive a smaller term. The daily component values can be further averaged to obtain their monthly, seasonal, and annual mean values. The results are summarized in the next section.

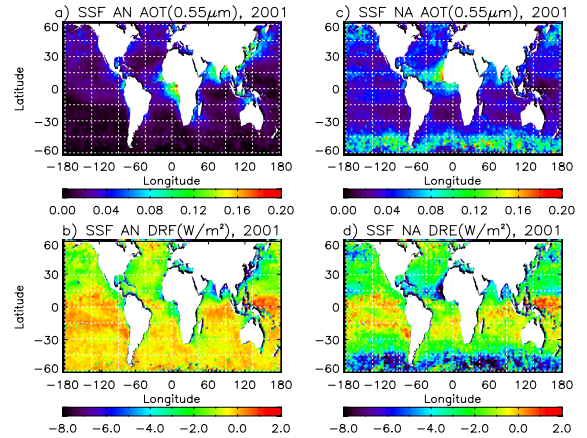


Figure 1. Global distribution of annual mean $0.55\mu\text{m}$ AOT (top) and TOA aerosol DRE/DRF (bottom) derived from the CERES/SSF data for anthropogenic (AN) and natural (NA) aerosol components.

4. RESULTS AND DISCUSSIONS

Figure 1 displays the global distributions of annual mean aerosol DRE/DRF and the corresponding AOTs for the anthropogenic and natural aerosol components.

Relatively strong negative forcing of anthropogenic aerosols are mainly located in the east coast of China, the Bay of Bengal, the Arabian Sea, and the west coast of central-south Africa, which is consistent with the enhanced aerosol loadings due to either bio-mass burning or industrial pollutions over these regions. The major negative DRE of natural aerosols occurs mainly over the west coast of Africa due to dust particles and over the oceans on the middle latitude of the SH and the high latitude of the NH due to sea salt. The global mean values of ΔF are -1.6W/m^2 for anthropogenic component and -3.6W/m^2 (-2.6W/m^2 of sea salt and -1.1W/m^2 of dust) for natural component and the corresponding AOT values are 0.027 for anthropogenic component and 0.053 (0.036 of sea salt and 0.016 of dust) for natural component.

In Figure 2, annual mean TOA aerosol DRE derived using the proposed approach from the SSF data of 2001 is compared with the calculation (Yu et al., 2003, 2004) from the Fu-Liou broadband radiation model (using the merged standard MODIS and GOCART aerosol fields). Their general patterns in global distribution compare reasonably well. Detailed comparison is performed over 13 selected regions over the globe and the results are summarized in Table 1. Except in regions 3 and 7 (due to less samples), the difference of SSF values and calculated values are less than 1.0W/m^2 , which are much smaller than their standard divisions (STD).

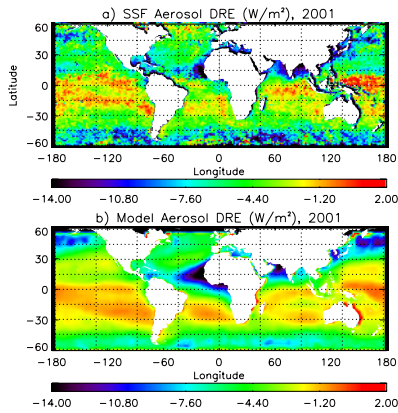


Figure 2. Comparison of annual mean TOA aerosol DRE of (a) SSF data and (b) Fu-Liou radiation model calculation.

Further comparison of our component aerosol DRE/DRF values with more model and observational estimates is given in Table 2. Our values for SS, DU, and SU are somewhat smaller than the GCM simulation. SU value is slightly larger than the recent model simulations and DU is slightly higher than the recent observations. Our OM value agrees well with the recent model simulations but lower than the GCM

value. Our value for BC, $+0.04\text{W/m}^2$, is much lower than the GCM and the recent model values. This is probably due to the uncertainty associated with our partitioning of BC through a subtraction of two big terms to derive a smaller term.

Regions		SSF (W/m^2)		Model (W/m^2)		ΔF_S $-\Delta F_M$
Lat ($^\circ$)	Lon ($^\circ$)	ΔF_S	STD	ΔF_M	STD	
30N-60N	90W-180W	-5.9	3.0	-6.3	2.9	0.44
30N-60N	0W-90W	-4.8	2.9	-5.6	2.1	0.88
30N-60N	0E-90E	-10.9	11.6	-4.2	3.6	-6.70
30N-60N	90E-180E	-7.6	6.4	-8.4	3.2	0.73
0N-30N	90W-180W	-4.3	2.8	-4.2	1.1	-0.07
0N-30N	0W-90W	-7.4	4.4	-7.6	3.1	0.25
0N-30N	0E-90E	-8.9	5.0	-5.7	4.4	-3.19
0N-30N	90E-180E	-5.4	4.7	-4.5	1.9	-0.94
0S-30S	90W-180W	-2.2	1.3	-3.0	0.3	0.84
0S-30S	0W-90W	-3.2	3.2	-3.6	1.9	0.45
0S-30S	0E-90E	-3.0	2.1	-3.7	1.8	0.68
0S-30S	90E-180E	-2.7	4.0	-3.2	1.1	0.52
30S-60S	180W-180E	-5.9	3.4	-5.6	1.7	-0.30
globe ocean		-5.2	4.2	-4.5	3.1	-0.70

Table 1. Comparison of annual mean TOA aerosol DRE (or ΔF) derived from the CERES/SSF satellite data and the Fu-Liou radiation model calculation over the global oceans and in 13 selected regions recommended by the Climate Change Science Program (CCSP) Working Group on Aerosol Properties and Their Impacts on Climate.

There are several major uncertainties associated with our estimates. First is caused by potential sub-pixel cloud contamination, the magnitude can be about 1.25W/m^2 (or 25%). This value is obtained by relax the strong clear condition from 99% to 95% in our selection of SSF pixels for the analysis (Zhao et al., 2005a, b). Second is the uncertainty in the derived total ΔF , which is mainly due to the error in the determination of \bar{F}^{-as} (Loeb and Kato, 2002) and the value can be up to 1W/m^2 (about 20% of our annual mean value) according to their estimation. The third is associated with the assumption in our partitioning which is about 5% for SS and SU, 10% for DU and OM, and 16% for BC as discussed in Section 3. Assuming the uncertainty associated with cloud contamination and derivation of total ΔF is independent, the final uncertainty for ΔF becomes

32%. Further assuming this 32% is carried over in the partition, the final uncertainty is 37% for SS and SU, 42% for DU and OM, and 48% for BC. The real uncertainties in our derived values of aerosol DRE/DRF are expected larger than our preliminarily estimates if errors associated with the CERES cloud screening scheme and the GOCART model simulation of the major aerosol components are included, which is out the scope of this study.

AC	ΔF (W/m ²)			
	SSF	GCM ¹	Recent Observations ²	Recent Models ³
BC	+0.04	+0.17	—	+0.15 — +0.45
OM	-0.48	-1.02	—	-0.15 — -0.65
SU	-1.09	-1.65	—	-0.21 — -0.96
DU	-1.09	-1.12	-0.80	—
SS	-2.55	-3.27	-4.85	—
AN	-1.64	-2.10	-0.76	—
NA	-3.56	-4.75	-5.65	—
Total	-5.20	-6.85	-3.8 — -6.5 (-5.5)	-2.3 — -4.7 (-3.2)

Table 2. Comparison of global and annual mean TOA aerosol DRE/DRF for the major aerosol components (AC) over ocean derived from the CERES/SSF data with other observational and model-based estimates. [Notes: ¹GCM values are taken from Haywood et al. (1999). ^{2, 3}A range is given for the total ΔF (taken from Yu et al., 2005) with the mean value in a parenthesis. The component values of observation are from Bellouin et al. (2005) while the model-based values are from Adams et al. (2001); Schulz et al. (2005); Takemura et al. (2005)].

In summary, Terra CERES/MODIS-SSF SW flux data have been combined with GOCART model output and a SSF/MODIS-GOCART merged total AOT product to derive TOA component aerosol DRE/DRF over the global oceans for clear-sky conditions through a two-step approach. The derived global means of total aerosol DRE/DRF over ocean in Spring, Summer, Fall, Winter, and annual average are respectively -6.09, -4.69, -4.38, -5.19, and -5.20W/m². These values agree well with the other 23 observational and model values collected in Yu et al. (2005). The derived annual mean values of component aerosol DRF over global oceans are summarized in Table 2.

ACKNOWLEDGMENTS

We would like to acknowledge the NASA CERES project and the DAAC of the NASA Langley for supplying the CERES/SSF data. Proofreading of the manuscript by Dr. Bob Kuligowski at the NESDIS/ORA is greatly appreciated. This research is funded by the NASA Radiation Program through grant RSP-0022-0005.

REFERENCES

- Adams, P. J., et al., General circulation model assessment of direct radiative forcing by the sulfate-nitrate-ammonium-water inorganic aerosol system, *J. Geophys. Res.*, **106**, 1097-1112, 2001.
- Bellouin, N., et al., Aerosol absorption over the clear-sky oceans deduced from POLDER-1 and AERONET observations, *Geophys. Res. Lett.*, **30**, doi:10.1029/2003GL017121, 2003.
- Bellouin, N., et al., Global estimate of aerosol direct radiative forcing from satellite measurements, *Nature*, in press, 2005.
- Boucher, O., et al., Intercomparison of models representing short-wave radiative forcing by sulfate aerosols, *J. Geophys. Res.*, **103**, 16,979-16,998, 1998.
- Boucher, O., and D. Tanré, Estimation of the aerosol perturbation to the Earth's radiative budget over oceans using POLDER satellite aerosol retrievals, *Geophys. Res. Lett.*, **27**, 1103-1106, 2000.
- Chin, M., et al., Atmospheric sulfur cycle simulated in the global model GOCART: Model description and global properties, *J. Geophys. Res.*, **105**, 24,671-24,687, 2000.
- Chin, M., et al., Tropospheric aerosol optical thickness from the GOCART model and comparison with satellite and sun photometer measurements, *J. Atmos. Sci.*, **59**, 461-483, 2002.
- Haywood, J. M., V. Ramaswamy, B. J. Soden, Tropospheric aerosol climate forcing in clear-sky satellite observations over the oceans, *Science*, **283**, 1299-1303, 1999.
- Kaufman, Y. J. et al., Aerosol anthropogenic component estimated from satellite data, *Geophys. Res. Lett.*, **32**, doi:10.1029/2005GL023125, 2005.
- Loeb, N. G., and S. Kato, Top-of-atmosphere direct radiative effect of aerosols over the tropical oceans from the Clouds and the Earth's Radiant Energy System (CERES) satellite instrument, *J. Climate*, **15**, 1474-1484, 2002.
- Loeb, N. G., and N. Manalo-Smith, Top-of-atmosphere direct radiative effect of aerosols over global oceans from merged CERES and MODIS observations, *J. Climate*, **18**, 3506-3526, 2005.
- Remer, L. A., and Y. J. Kaufman, Aerosol effect on the distribution of solar radiation over the clear-sky global oceans derived from four years of MODIS retrievals, *Atmos. Chem. Phys. Discuss.*, **5**, 5007-5038, 2005.
- Schulz, M., et al., Radiative forcing by aerosols as derived from the AeroCom present-day and pre-industrial simulations, *Atmos. Chem. Phys. Discuss.*, submitted, 2005.

- Takemura, T., et al., Simulation of climate response to aerosol direct and indirect effects with aerosol transport-radiation model, *J. Geophys. Res.*, **110**, D022202, doi:10.1029/2004JD005029, 2005.
- Yu, H., et al., Annual cycle of global distributions of aerosol optical depth from integration of MODIS retrievals and GOCART model simulations, *J. Geophys. Res.*, **108**, D34128, doi:10.1029/2002JD002717, 2003.
- Yu, H., et al., The direct radiative effect of aerosols as determined from a combination of MODIS retrievals and GOCART simulations, *J. Geophys. Res.*, **109**, D03206, doi:10.1029/2003JD003914, 2004.
- Yu, H., et al., A review of measurement-based assessment of aerosol direct radiative effect and forcing, *Atmos. Chem. Phys. Discuss.*, **5**, 7647-7768, 2005. SRef-ID: 1680-7375/acpd/2005-5-7647.
- Zhang, J., et al., Shortwave aerosol radiative forcing over cloud-free oceans from Terra: 1. Angular models for aerosols, *J. Geophys. Res.*, doi:10.1029/2004JD005008, 2005a.
- Zhang, J., et al., Shortwave aerosol radiative forcing over cloud-free oceans from Terra: 2. Seasonal and global distributions, *J. Geophys. Res.*, doi:10.1029/2004JD005009, 2005b.
- Zhao, T. X.-P., et al., Comparison and analysis of two aerosol retrievals over the ocean in the Terra/CERES-MODIS single scanner footprint (SSF) data: Part I – global evaluation, *J. Geophys. Res.*, doi:10.1029/2005JD005851, 2005a.
- Zhao, T. X.-P., et al., Comparison and analysis of two aerosol retrievals over the ocean in the Terra/CERES-MODIS single scanner footprint (SSF) data: Part II – regional evaluation, *J. Geophys. Res.*, doi:10.1029/2005JD005852, 2005b.